Assessment of existing and introduction of a new and robust pragmatic definition of the representative volume element

H. Moussaddy, D. Therriault and M. Lévesque*

Laboratory for Multiscale Mechanics (LM2), Department of Mechanical Engineering, École Polytechnique de Montréal, C.P. 6079, succ. Centre-ville, Montréal, Québec, Canada H3C3A7

* Corresponding author: martin.levesque@polymtl.ca

Abstract

Accurate numerical homogenization necessitates the thorough determination of the Representative Volume Element (RVE). This paper demonstrates that common techniques, based on studying the convergence rate of the effective properties with respect to the volume element size, are invalid for a certain range of microstructures and yield erroneous estimates of their effective properties. Different RVE determination methods were tested for the case of composites reinforced by randomly oriented and high aspect ratio fibers. Following the failure of traditional RVE determination methods, we proposed a new RVE determination criterion that is not based on the average property stability, but its statistical variations. Our new proposed criterion has been shown to be more accurate than other criteria in computing the effective properties of composites for aspect ratios up to 60. Moreover, the proposed criterion does not necessitate a convergence study over the volume element size, hence reducing considerably the RVE determination cost. Finally, our work questions the validity of many published works dealing with composites including heterogeneities of high aspect ratios.

Keywords: *numerical homogenization, representative volume element, finite element, random orientation, fiber composites.*

1 Introduction

Three-dimensional (3D) numerical homogenization can deliver accurate effective properties for composites with arbitrary microstructures. Several authors have studied specific microstructures, such as randomly dispersed spheres [1] or aligned fibers [2], using 3D numerical homogenization methods based on the Finite Element (FE) and Fast Fourier Transforms (FFT). However, only a few works on Randomly Oriented Fiber Reinforced Composites (ROFRCs) are reported in the literature and are limited, due to computational challenges, to low volume fractions (e.g., Lusti and Gusev up to 1% [3], Mortazavi *et al.* at 1% and 3% [4]) and low fibers aspect ratios $\mathrm{AR} = l_{fiber} / d_{fiber}$ where l_{fiber} is the fiber length and d_{fiber} is the fiber radius (e.g., $\mathrm{AR} = 5$ in Bohm *et al.* [5], $\mathrm{AR} \leq 15$ in Kari *et al.* [6]). Most importantly, most ROFRCs numerical studies were conducted without a rigorous determination of the Representative Volume Element (RVE). In the sequel, the "apparent properties" refer to the properties of an arbitrary volume element, whereas "effective properties" refer to that of the RVE.

The RVE determination is of paramount importance to numerical homogenization methods since it ensures accurate estimations of the effective properties. The RVE is classically defined as a volume of the material large enough to represent the material macroscopic behavior, i.e. a volume that yields the same effective properties as the bulk composite. The volume of the material is hereby quantified by the number of heterogeneities/fibers that are represented within. Larger volume elements include larger number of heterogeneities. The process of establishing the RVE is traditionally based on

the criterion of apparent property stability, within a tolerance, when incrementing the number of heterogeneities in the composite volume [7, 8]. However, no studies have verified the validity of this method for the case of heterogeneities with high aspect ratios (AR>10). The RVE determination process generally requires the numerical homogenization of a large number of random microstructure realizations (i.e., 3D virtual images of ROFRC microstructures) for a series of volumes with an incrementing number of heterogeneities (e.g., number of fibers represented in the ROFRC virtual image) [8]. The high computational cost of the RVE determination process for ROFRCs has lead many authors to ignore the elementary RVE concept in their studies [3-6]. As a result, one could question the accuracy of the results in most of the published papers dealing with ROFRCs.

The objective of this paper is to rigorously study the RVE determination process for the case of ROFRCs with different aspect ratios. Different methods of RVE determination were tested through a series of FE numerical simulations of a ROFRC with 5% volume fraction of fibers and for different aspect ratios. The validity of the different RVE determination methods was assessed by comparing their corresponding effective properties to those of very large volumes. To the authors' knowledge, the RVE determination has neither been rigorously analyzed nor even attempted, yet, for ROFRCs.

The challenges for each step of a numerical homogenization process are first reviewed. In Section 3, several RVE determination criteria and methods are presented. Section 4 describes briefly the numerical simulations and the parameters used in this study. Section 5 contains a comparison between the results of different RVE determination methods. Finally, the main conclusions of this work are listed in Section 6.

2 Background

Most numerical homogenization studies follow the methodology described below. First, a 3D image of a random microstructure is generated (Section 2.1). Then, the 3D image is discretized following the technique of FE or FFT (Section 2.2). Boundary conditions are then enforced on the model (Section 2.3), followed by the computation of the microstructure apparent properties (Section 2.4). Several techniques can help reducing the computational cost of the numerical homogenization process (Section 2.5). Finally, the RVE is determined by analyzing the numerical results of several random microstructures (Section 2.6).

2.1 Random microstructure generation

The first step in numerical homogenization of ROFRCs is to generate a 3D image of a microstructure where the fibers are randomly positioned and oriented. Different methods are commonly used for constructing random microstructure volumes, namely: random sequential adsorption (RSA) [9, 10], Monte-Carlo simulations [7], molecular dynamics simulations [1, 11], random-walk methods [12] and experimental image reconstruction techniques [13]. The RSA algorithm [9, 10], presented herein, has been the most commonly used method for random microstructures generation due to its simplicity. Among the other above-mentioned methods, only the random-walk method has been shown recently to generate more compact packings for ROFRCs [12]. However, the method is limited to bended fibers only, which are not desired in our case since this work aims at comparing the computed effective properties with that estimated from micromechanical analytical models (e.g., Mori-Tanaka [14]) that assume straight fibers.

The RSA method consists of sequentially adding fibers into a volume, while checking for contact interferences with all previously generated fibers, until the target volume fraction is reached. If a newly added fiber overlaps with another fiber, it is removed and then repositioned randomly in the same volume. This repositioning operation is repeated until the new fiber location is free from interferences. However, achievable microstructures by RSA are limited to low volume fractions, due to fiber interpenetration, also known as the jamming limit [9]. The RSA process becomes even more complicated for high aspect ratio fibers because they have more probability to interfere with each other. This can be observed in the percolation theory where it is predicted that longer and randomly oriented fibers have an increased probability of forming a connected network [15]. This explains partially why ROFRCs efforts have been limited to low aspect ratios. Kari *et al.* [6] proposed a modification to the original RSA scheme to overcome the jamming limit by adding smaller fibers to fill-up the volume after reaching the jamming limit at a given initial fiber size. However, discrepancies in aspect ratios and sizes of fibers in the same microstructure induce very refined discretizations of microstructures, increasing substantially the computational cost. Therefore, there is still a need to improve the RSA method for randomly oriented straight fibers in order to extend the range of achievable volume fractions and aspect ratios. An original modification to the RSA scheme is proposed in Appendix A where a displacement is imposed on added fibers that interfere with existing fibers.

2.2 Numerical solution methods and geometry discretization

The FE and the FFT methods are among the most used numerical methods to estimate the effective properties of composite microstructures. The latter has been reported by Moulinec and Suquet [16, 17] and has been recently used in a study on the effective properties of sphere reinforced composites [1]. The FFT method requires uniform discretization of a three dimensional microstructure image into equal size cubic volumes (i.e., voxels) in order to enjoy the computational efficiency of FFT. The principal advantage of this method is that it avoids the meshing difficulties usually associated with FE and can be fully automated, by opposition to FE where user input is required in most cases. However, the number of voxels required to represent adequately the geometry of high aspect ratio fibers becomes very important and leads to very large computational costs. The FE allows for a non-uniform distribution of elements (i.e., free meshes) permitting different levels of mesh refinements in different parts of the microstructure. Moreover, different types and shapes of elements can be used to accurately represent the fiber circular cross-section. When the meshing is complete, boundary conditions are enforced on the meshing as described next.

2.3 Boundary conditions

For an infinitely large volume, the effective properties are independent of the applied boundary conditions [18, 19]. Therefore, regardless of the enforced boundary conditions, all apparent properties should converge to the effective properties when increasing the number of heterogeneities. The main criterion that should be driving the choice of boundary conditions is the convergence rate of the apparent properties towards the

effective properties. It has been demonstrated [8] that periodic boundary conditions converge towards the effective properties for smaller volumes than uniform tractions or displacements. By definition, periodic boundary conditions are implemented into FFT methods [17]. However, the implementation of periodic boundary conditions into FE models is more challenging. Periodic boundary conditions application in FE packages can be achieved through the elimination method using Multiple-Point Constraints (MPC). In order to exactly meet the periodicity of the displacement field, the microstructure must be periodic and the meshes on opposite faces of the volume element must be identical. Following the meshing, all matching nodes displacements are coupled through the periodic boundary conditions equation:

$$\boldsymbol{u}_{(x_2)} - \boldsymbol{u}_{(x_1)} = \mathbf{E} \cdot \left(\boldsymbol{x}_2 - \boldsymbol{x}_1 \right), \tag{1}$$

where $\boldsymbol{u}_{(xi)}$ is the displacement vector of the node at location $\boldsymbol{x_i}$, $\boldsymbol{x_1}$ and $\boldsymbol{x_2}$ are the coordinates of two matching nodes on opposite faces of the cubic volume and **E** is the applied macroscopic strain (set by the user). The reader is referred to [20] for a more detailed discussion on periodic boundary conditions implementation in numerical homogenization problems. Following the boundary conditions enforcement, the numerical model is solved and the apparent elastic properties are consequently determined as described in the next section.

2.4 Computation of the elastic properties

The apparent elastic tensor $\widetilde{\mathbf{C}}$ of a volume element is computed through:

$$\boldsymbol{\Sigma} = \widetilde{\mathbf{C}} \ : \ \mathbf{E}, \tag{2}$$

where $\boldsymbol{\Sigma}$ is the macroscopic stress tensor. $\boldsymbol{\Sigma}$ and $\mathbf{E}$ are defined as :

$$\boldsymbol{\Sigma} = \left\langle \boldsymbol{\sigma}(\boldsymbol{x}) \right\rangle_V, \tag{3.a}$$

$$\mathbf{E} = \left\langle \varepsilon(\boldsymbol{x}) \right\rangle_V, \tag{3.b}$$

where $\boldsymbol{\sigma}(\boldsymbol{x})$ and $\varepsilon(\boldsymbol{x})$ are the local stress and strain fields, respectively. Angle brackets $\langle . \rangle$ indicate an averaging over the volume $\boldsymbol{V}$ as

$$\left\langle \boldsymbol{\sigma}(\boldsymbol{x}) \right\rangle_V = \frac{1}{V} \int_V \boldsymbol{\sigma}(\boldsymbol{x}) dV. \tag{4}$$

For discretized elements, angle brackets $\langle . \rangle$ indicate a volume averaging of the discrete field:

$$\left\langle \boldsymbol{\sigma}_i \right\rangle_V = \frac{1}{V} \sum V_i \, \boldsymbol{\sigma}_i, \tag{5}$$

where V_i and $\boldsymbol{\sigma}_i$ are the volume and stress attributed to the i^{th} finite element (or integration point).

In order to show explicitly how the effective elastic tensor $\widetilde{\mathbf{C}}$ is calculated, the modified Voigt (Mandel) notation is used by which Eq. (2) becomes:

$$\begin{bmatrix} \Sigma_{11} \\ \Sigma_{22} \\ \Sigma_{33} \\ \sqrt{2}\Sigma_{12} \\ \sqrt{2}\Sigma_{13} \\ \sqrt{2}\Sigma_{23} \end{bmatrix} = \begin{bmatrix} \widetilde{C}_{1111} & \widetilde{C}_{1122} & \widetilde{C}_{1133} & \sqrt{2}\widetilde{C}_{1112} & \sqrt{2}\widetilde{C}_{1113} & \sqrt{2}\widetilde{C}_{1123} \\ \widetilde{C}_{2211} & \widetilde{C}_{2222} & \widetilde{C}_{2233} & \sqrt{2}\widetilde{C}_{2212} & \sqrt{2}\widetilde{C}_{2213} & \sqrt{2}\widetilde{C}_{2223} \\ \widetilde{C}_{3311} & \widetilde{C}_{3322} & \widetilde{C}_{3333} & \sqrt{2}\widetilde{C}_{3312} & \sqrt{2}\widetilde{C}_{3313} & \sqrt{2}\widetilde{C}_{3323} \\ \sqrt{2}\widetilde{C}_{1211} & \sqrt{2}\widetilde{C}_{1222} & \sqrt{2}\widetilde{C}_{1233} & 2\widetilde{C}_{1212} & 2\widetilde{C}_{1213} & 2\widetilde{C}_{1223} \\ \sqrt{2}\widetilde{C}_{1311} & \sqrt{2}\widetilde{C}_{1322} & \sqrt{2}\widetilde{C}_{1333} & 2\widetilde{C}_{1312} & 2\widetilde{C}_{1313} & 2\widetilde{C}_{1323} \\ \sqrt{2}\widetilde{C}_{2311} & \sqrt{2}\widetilde{C}_{2322} & \sqrt{2}\widetilde{C}_{2333} & 2\widetilde{C}_{2312} & 2\widetilde{C}_{2313} & 2\widetilde{C}_{2323} \end{bmatrix} \begin{bmatrix} E_{11} \\ E_{22} \\ E_{33} \\ \sqrt{2}E_{12} \\ \sqrt{2}E_{13} \\ \sqrt{2}E_{23} \end{bmatrix}. \quad (6)$$

In order to obtain all the terms of the apparent elasticity tensor $\widetilde{\mathbf{C}}$, each FE model can be solved 6 times using 6 orthogonal deformation states, namely:

$$\mathbf{E}^1 = \begin{bmatrix} \varepsilon \\ 0 \\ 0 \\ 0 \\ 0 \\ 0 \end{bmatrix}; \ \mathbf{E}^2 = \begin{bmatrix} 0 \\ \varepsilon \\ 0 \\ 0 \\ 0 \\ 0 \end{bmatrix}; \ \mathbf{E}^3 = \begin{bmatrix} 0 \\ 0 \\ \varepsilon \\ 0 \\ 0 \\ 0 \end{bmatrix}; \ \mathbf{E}^4 = \begin{bmatrix} 0 \\ 0 \\ 0 \\ \varepsilon\sqrt{2} \\ 0 \\ 0 \end{bmatrix}; \ \mathbf{E}^5 = \begin{bmatrix} 0 \\ 0 \\ 0 \\ 0 \\ \varepsilon\sqrt{2} \\ 0 \end{bmatrix}; \ \mathbf{E}^6 = \begin{bmatrix} 0 \\ 0 \\ 0 \\ 0 \\ 0 \\ \varepsilon\sqrt{2} \end{bmatrix}. \quad (7)$$

Each deformation state is applied separately on the non-deformed FE model. By implementing (7) in (6), each deformation state results in a single column of the apparent elastic tensor $\widetilde{\mathbf{C}}$ in its matrix notation. Consequently, all 6 columns of the apparent elasticity tensor can be calculated. Conversely, if tractions based boundary conditions were to be applied, six orthogonal states of applied tractions would be needed to

determine the 36 terms of the compliance tensor $\widetilde{\mathbf{S}}$ in its matrix notation. It should be noted that for infinitely large volume elements, at most 21 constants need to be determined due to the symmetry of the stress and strain tensors.

It is well established that a random orientation distribution of fibers should lead to isotropic effective properties [21]. Therefore, only two elastic parameters are sufficient to describe the effective behavior of the composite. Assuming the isotropy of the volume element, the apparent bulk modulus $\tilde{k}$ and shear modulus $\widetilde{G}$ can be calculated from $\widetilde{\mathbf{C}}$ using the isotropy projectors resulting in the following equations expressed using the Einstein summation convention:

$$\tilde{k} = \frac{\widetilde{\mathrm{C}}_{iijj}}{9}, \tag{8.a}$$

$$\widetilde{G} = \frac{3\ \widetilde{\mathrm{C}}_{ijij} - \widetilde{\mathrm{C}}_{iijj}}{30}. \tag{8.b}$$

It should be noted that only two loading cases are required to estimate $\tilde{k}$ and $\widetilde{G}$. However, we performed the 6 load cases, stated in Eq.(7), required to obtain the full stiffness tensor in order to study its deviation from isotropy (see Section 3.1.1)

2.5 FE computation techniques

ROFRCs discretized microstructures usually require large FE models with a very high number of degrees of freedom (DOF). With 15 randomly oriented fibers of aspect ratio 5 and a volume fraction of 15%, Bohm *et al.* [5] obtained a 130,000 nodes FE model

(390,000 DOF). The number of DOF substantially increases for higher aspect ratios of fibers. The computational memory required for the solution of the corresponding FE models cannot be handled by typical workstation computers and classical solving methods. However, specific techniques can reduce the memory requirements and computational time of the FE computations. One important technique to significantly reduce the computational cost is the use of iterative solvers. Iterative solvers such as the Krylov subspace methods (e.g. pre-conditioned conjugate gradient) can significantly reduce the memory required as well as the computational time when compared to the direct sparse solver. These types of solvers are most efficient when used for block-like structures with high number of DOF (i.e., over a million) [22], as for the case of ROFRC volume elements. Most commercial FE packages (e.g., Abaqus/Standard v6.10, ANSYS v13.0) have iterative solvers already implemented but must be specified by the user. However, certain element types, contact or non-linearity of material properties or geometries can lead to ill-conditioned models which will slowly or even fail to converge.

Another important aspect of large model computation is parallelization. Thread-based-parallelization can be utilized to parallelize independent tasks and loops. Moreover, Message Passing Interface (MPI) based parallelization in domain decomposition methods [23-25] can be utilized in parallelizing the model on a computer cluster. FE Tearing and Interconnecting method (FETI) [24, 25] is a domain decomposition method which breaks down the model into subdomains that share only interfaces. Forces and displacements at the interfaces of subdomains are determined iteratively in an automated process without any user intervention. The N subdomains are solved in N different processes that communicate through the MPI. The combination of iterative solvers and parallelization

schemes can help widen the range of achievable volume fractions and fibers aspect ratios for ROFRCs. However, not every combination of parallelization scheme and solver is possible. For more information about FE solvers and parallelization, the reader is referred to [26].

2.6 RVE determination

2.6.1 RVE definitions

The validity of the numerical homogenization relies on the notion of the RVE. As originally described by Hill [18] and later by others [19, 27, 28], the "theoretical RVE" refers to a sample that is large enough 1) to include a sampling of all microstructural heterogeneities that occur in the composite and 2) to deliver effective properties that are independent of boundary conditions. The theoretical RVE definition is simple in its physical meaning but remains challenging to determine in practice. A more practical RVE definition is found in the framework of homogenization in which a "numerical RVE" is defined as the smallest volume element that has the same target property/behavior as the full scale material [7, 8]. While the theoretical RVE is specific for the microstructure under study (e.g., volume fraction, contrast of properties, heterogeneities shapes, dispersion and orientation), the numerical RVE is in addition specific to the targeted property/behavior (e.g., bulk modulus, shear modulus, thermal properties) [8, 29-31]. The numerical RVE definition is more interesting than that of a theoretical RVE from a practical standpoint. Numerical RVE should result in smaller volumes while still satisfying the homogenization primary objective of having accurate effective properties.

2.6.2 Numerical RVE determination

A numerical RVE is usually characterized by the number of represented heterogeneities in the volume. The number of heterogeneities that are required in a RVE is estimated through the verification of specific criteria. Those RVE determination criteria should, necessarily, be able to identify a RVE with accurate properties and, ideally, with the smallest volume element as possible. Selecting appropriate RVE criteria is not trivial. Inadequately selected criteria can lead either to a volume smaller than the RVE, hence yielding erroneous results, or to a very large RVE that induces prohibitively large computational costs.

The first numerical RVE criteria reported in the literature relied on the stability of the apparent properties of volume elements over increments of the number of heterogeneities in the volume [7]. Gusev [7] used this determination criterion to determine the RVE of randomly dispersed spheres reinforced composites. Later on, Kanit *et al.* [8] have presented an algorithm to determine the RVE defined not only by its number of represented heterogeneities, but also by the number of random realizations of the volume element required to have confidence in the results. In [8], it is shown that by performing a certain number of realizations with fewer heterogeneities, it is possible to obtain the same property as that of a single and larger RVE and with the same accuracy. However, this was shown to be untrue for small volume sizes, as there is a bias caused by deterministic size effects (e.g., boundary effects) which cannot be eliminated through ensemble averaging [8]. Hence the numerical RVE is defined as the representative ensemble of r_{RVE} realizations, with the fewest number of heterogeneities n_{RVE}, which yields by average the composite effective properties, within a given tolerance.

Several determination criteria have been used in the literature [1, 8, 30-34] to determine RVE parameters (n_{RVE}, r_{RVE}). To the author's knowledge, only one criterion was used, under several forms, to determine the number realizations required r_{RVE} [1, 30-32]. The criterion aims at the determination of the ensemble size *r* of realizations that will give satisfactory confidence in the average properties. Precisely, the criterion ensures that the ensemble of realizations average property should be representative, within a tolerance, of the average of the whole statistical population of possible microstructures at that number of heterogeneities. In contrast, several different criteria were used to determine the number of heterogeneities in the RVE n_{RVE}. The first, and most commonly used, criterion is that of effective property stability over increments of number of heterogeneities in the volume [1, 6, 7, 20, 31, 33]. The only difference from the early definition of the criterion, used by Gusev [7], is that the stability criterion is applied to the ensemble average properties and not to a single volume element for each volume size. Another criterion was based on increasing the number of heterogeneities until the bounds of effective properties, issued from uniform displacement and uniform traction boundary conditions, are close within a tolerance [34]. Even though this criterion is the only one to provide exact bounds and errors for the effective properties, uniform displacement and traction boundary conditions are too distant apart for high contrasts of constituents' properties. It was demonstrated in [34] that uniform displacement and traction boundary conditions converge faster for a free-form volume element, whose side does not intersect with heterogeneities, than for a cubic volume element which intersects heterogneities. Whether the refined bounds converge quicker than periodic boundary conditions or not is

left for future studies since the generation of free form VE for the microstructures studied herein would require significant amount of work. A third criterion to determine n_{RVE} is that of enforcing that the variation/deviation of the targeted property over all realizations is within a tolerance of their average [33, 34]. Indeed, very low scattering of the effective properties would be observed if an arbitrarily large number of heterogeneities were included in the volume. Other RVE size determination criteria were developed based on geometrical and statistical properties of the realizations [33], but are not directly related to the effective properties and, hence, are not included in this study.

The process of determining the RVE parameters is therefore usually done using a two-fold convergence. First the number of realizations is incremented until satisfying the first criterion and determining r_{RVE}. Second, the volume size is incremented until satisfaction of the second criterion and determining n_{RVE}. This process usually leads to a very large number of FE models to evaluate, among which only one set will be defined as the RVE. Furthermore, no studies have verified the validity of the different criteria results, especially for the case of heterogeneities with high aspect ratios. For example, the stability criterion verifies only the convergence rate of the targeted property over size increments without any indication on the effective properties accuracy. There might be cases where the property converges very slowly over size increments and the numerical stability criterion is not strict enough to ensure that the property of interest has effectively stabilized. As a result, premature convergence towards false results is possible. In this study, an attempt was made to evaluate the accuracy of the stability criterion, but also to suggest and assess the robustness of new methods of RVE determination.

3 RVE determination methods

Several RVE determination methods were tested to determine both RVE parameters (n_{RVE}, r_{RVE}). Each method consists of an algorithm involving two RVE determination criteria. In the following, the determination criteria are first presented, followed by the listing of the general algorithm for all determination methods.

3.1 Determination criteria

Two groups of determination criteria were tested to compute the RVE parameters (n_{RVE}, r_{RVE}). The first group lists the number of realizations r_{RVE} determination criteria, while the second group lists number of fibers n_{RVE} determination criteria. While the bulk modulus is studied below for illustration purposes, the criteria can be applied to any elastic property.

3.1.1 Ensemble size criteria

An ensemble size criterion aims at ensuring that the ensemble of realizations is large enough to have confidence in the ensemble average apparent properties. Two criteria are used: the confidence interval criterion and the ensemble isotropy criterion.

Confidence criterion: This criterion has been used under different forms in several RVE determination studies [1, 8, 32]. The criterion states that the ensemble size is satisfactory if the confidence interval relative error is within a certain tolerance, namely:

$$\zeta_{\text{con}} = \frac{I_{\tilde{k}}^{95\%} / 2}{\bar{k}_n^r} \leq tol \tag{9}$$

where $I_{\tilde{k}}^{95\%}$ is the 95% confidence interval of the apparent bulk moduli, tol is the fixed tolerance, and $\overline{k}_n^r$ represents the arithmetic averaging of the apparent bulk moduli over the r realizations with n fibers each.

Ensemble isotropy criterion: This criterion imposes the condition that the ensemble average properties should have the same material symmetry as the full scale material, which is isotropy in our case. Using this criterion, individual realizations should not be necessarily isotropic, but the average stiffness tensor of the representative ensemble of realizations should be. The average stiffness tensor isotropy should always be true for an arbitrarily large ensemble of realizations since the theoretical orientation averaging of the stiffness or compliance tensor of even a single fiber composite over all orientations exhibits isotropic behavior. Several isotropy indices can be found [35, 36] in the literature but none of them provides a percentage error measurement. It is therefore not trivial to define a range in which the isotropy index provides an acceptable isotropy. Moreover, these indices collapse the whole elasticity matrix into one single index value. This operation can be practical in most cases, but may lead to inaccurate isotropy measurements.

A new isotropy error is hereby proposed that computes an error for each non-zero term of the stiffness matrix. For a single random microstructure, the isotropy error matrix is given by:

$$\Lambda = \begin{bmatrix} \frac{\widetilde{C}_{11} - C_{11}^{(\tilde{k}^r, \tilde{G}^r)}}{C_{11}^{(\tilde{k}^r, \tilde{G}^r)}} & \frac{\widetilde{C}_{12} - C_{12}^{(\tilde{k}^r, \tilde{G}^r)}}{C_{12}^{(\tilde{k}^r, \tilde{G}^r)}} & \frac{\widetilde{C}_{13} - C_{13}^{(\tilde{k}^r, \tilde{G}^r)}}{C_{13}^{(\tilde{k}^r, \tilde{G}^r)}} & 0 & 0 & 0 \\ \frac{\widetilde{C}_{21} - C_{21}^{(\tilde{k}^r, \tilde{G}^r)}}{C_{21}^{(\tilde{k}^r, \tilde{G}^r)}} & \frac{\widetilde{C}_{22} - C_{22}^{(\tilde{k}^r, \tilde{G}^r)}}{C_{22}^{(\tilde{k}^r, \tilde{G}^r)}} & \frac{\widetilde{C}_{23} - C_{23}^{(\tilde{k}^r, \tilde{G}^r)}}{C_{23}^{(\tilde{k}^r, \tilde{G}^r)}} & 0 & 0 & 0 \\ \frac{\widetilde{C}_{31} - C_{31}^{(\tilde{k}^r, \tilde{G}^r)}}{C_{31}^{(\tilde{k}^r, \tilde{G}^r)}} & \frac{\widetilde{C}_{32} - C_{32}^{(\tilde{k}^r, \tilde{G}^r)}}{C_{32}^{(\tilde{k}^r, \tilde{G}^r)}} & \frac{\widetilde{C}_{33} - C_{33}^{(\tilde{k}^r, \tilde{G}^r)}}{C_{33}^{(\tilde{k}^r, \tilde{G}^r)}} & 0 & 0 & 0 \\ 0 & 0 & 0 & \frac{\widetilde{C}_{44} - C_{44}^{(\tilde{k}^r, \tilde{G}^r)}}{C_{44}^{(\tilde{k}^r, \tilde{G}^r)}} & 0 & 0 \\ 0 & 0 & 0 & 0 & \frac{\widetilde{C}_{55} - C_{55}^{(\tilde{k}^r, \tilde{G}^r)}}{C_{55}^{(\tilde{k}^r, \tilde{G}^r)}} & 0 \\ 0 & 0 & 0 & 0 & 0 & \frac{\widetilde{C}_{66} - C_{66}^{(\tilde{k}^r, \tilde{G}^r)}}{C_{66}^{(\tilde{k}^r, \tilde{G}^r)}} \end{bmatrix}, \quad (10)$$

and for an ensemble of *r* realizations, the isotropy error matrix is expressed by:

$$\Lambda^{\mathrm{r}} = \begin{bmatrix} \dfrac{\overline{\mathrm{C}}^{\mathrm{r}}_{11} - \mathrm{C}^{(\bar{k}^r,\bar{G}^r)}_{11}}{\mathrm{C}^{(\bar{k}^r,\bar{G}^r)}_{11}} & \dfrac{\overline{\mathrm{C}}^{\mathrm{r}}_{12} - \mathrm{C}^{(\bar{k}^r,\bar{G}^r)}_{12}}{\mathrm{C}^{(\bar{k}^r,\bar{G}^r)}_{12}} & \dfrac{\overline{\mathrm{C}}^{\mathrm{r}}_{13} - \mathrm{C}^{(\bar{k}^r,\bar{G}^r)}_{13}}{\mathrm{C}^{(\bar{k}^r,\bar{G}^r)}_{13}} & 0 & 0 & 0 \\ \dfrac{\overline{\mathrm{C}}^{\mathrm{r}}_{21} - \mathrm{C}^{(\bar{k}^r,\bar{G}^r)}_{21}}{\mathrm{C}^{(\bar{k}^r,\bar{G}^r)}_{21}} & \dfrac{\overline{\mathrm{C}}^{\mathrm{r}}_{22} - \mathrm{C}^{(\bar{k}^r,\bar{G}^r)}_{22}}{\mathrm{C}^{(\bar{k}^r,\bar{G}^r)}_{22}} & \dfrac{\overline{\mathrm{C}}^{\mathrm{r}}_{23} - \mathrm{C}^{(\bar{k}^r,\bar{G}^r)}_{23}}{\mathrm{C}^{(\bar{k}^r,\bar{G}^r)}_{23}} & 0 & 0 & 0 \\ \dfrac{\overline{\mathrm{C}}^{\mathrm{r}}_{31} - \mathrm{C}^{(\bar{k}^r,\bar{G}^r)}_{31}}{\mathrm{C}^{(\bar{k}^r,\bar{G}^r)}_{31}} & \dfrac{\overline{\mathrm{C}}^{\mathrm{r}}_{32} - \mathrm{C}^{(\bar{k}^r,\bar{G}^r)}_{32}}{\mathrm{C}^{(\bar{k}^r,\bar{G}^r)}_{32}} & \dfrac{\overline{\mathrm{C}}^{\mathrm{r}}_{33} - \mathrm{C}^{(\bar{k}^r,\bar{G}^r)}_{33}}{\mathrm{C}^{(\bar{k}^r,\bar{G}^r)}_{33}} & 0 & 0 & 0 \\ 0 & 0 & 0 & \dfrac{\overline{\mathrm{C}}^{\mathrm{r}}_{44} - \mathrm{C}^{(\bar{k}^r,\bar{G}^r)}_{44}}{\mathrm{C}^{(\bar{k}^r,\bar{G}^r)}_{44}} & 0 & 0 \\ 0 & 0 & 0 & 0 & \dfrac{\overline{\mathrm{C}}^{\mathrm{r}}_{55} - \mathrm{C}^{(\bar{k}^r,\bar{G}^r)}_{55}}{\mathrm{C}^{(\bar{k}^r,\bar{G}^r)}_{55}} & 0 \\ 0 & 0 & 0 & 0 & 0 & \dfrac{\overline{\mathrm{C}}^{\mathrm{r}}_{66} - \mathrm{C}^{(\bar{k}^r,\bar{G}^r)}_{66}}{\mathrm{C}^{(\bar{k}^r,\bar{G}^r)}_{66}} \end{bmatrix}, \quad (11)$$

where $\mathbf{C}^{(\tilde{k},\tilde{G})}$ is the isotropic stiffness matrix recalculated from the apparent elastic properties $\tilde{k}$ and $\tilde{G}$ and $\mathbf{C}^{(\bar{k},\bar{G})}$ is the isotropic stiffness matrix recalculated from the average apparent elastic properties $\bar{k}$ and $\bar{G}$.

The criterion dictates that the maximum term of the isotropy error matrix should be lower than a fixed tolerance:

$$\zeta_{\mathrm{iso}} = \max\left(\left|\Lambda^r\right|\right) \leq tol, \quad (12)$$

where $\max\left(\left|\Lambda^r\right|\right)$ indicates the maximum value of the matrix components.

3.1.2 Volume size criteria

Stability criterion: The property stability criterion is the most commonly used RVE determination criterion. It aims at the determination of the point of convergence of the target property when the number of heterogeneities is increased. Thus, we propose a generalized form of the stability criterion for an arbitrary increment of the number of fibers represented. To reach stability, the criterion states that the convergence rate of the bulk modulus should be within a certain tolerance:

$$\delta_{\text{stab}} = \frac{\left| \overline{k}_{n_2}^{r_2} - \overline{k_{n_1}^{r_1}} \right|}{\overline{k}_{n_2}^{r_2}} \times \left(\frac{\Delta n}{n_2 - n_1} \right) \leq tol \,, \tag{13}$$

where n_2 is larger than n_1, and Δn indicates the chosen reference step size. The ratio between Δn and $n_2 - n_1$ is hereby proposed to generalize the stability criterion for an arbitrary choice of volumes n_1 and n_2. The criterion's ability to determine accurately the RVE value depends on the choice of the tolerance value and of the reference volume step size Δn. Even though this criterion works well for microstructures with randomly dispersed spheres [1, 7], or grains [8], the microstructure of ROFRCs with high aspect ratios fibers were not tested and should provide more insight into the problems that can be faced.

Deviation criterion: The standard deviation of the target property is an indicator of the scatter in the ensemble of realizations. When the number of fibers increases, lower property variations should be observed. Theoretically, no variations should be observed

when the RVE is reached since the latter is typical of the whole microstructure. In this perspective, the RVE can be identified by fixing a maximum deviation tolerance for an ensemble of realizations:

$$\delta_{\text{dev}} = \frac{s_n^r}{\bar{k}_n^r} \leq tol, \tag{14}$$

where s_n^r is the standard deviation of the target property for an ensemble *r* with *n* fibers in each volume.

Averaging variations criterion (new): All previous criteria were based on the arithmetic mean of the apparent target property for the ensemble. The arithmetic mean value $\bar{k}_n^r$ of the apparent properties of the realizations was considered as the overall ensemble property. Here we consider two averages of the ensemble properties, namely the arithmetic and harmonic means:

$$\bar{k}^r = \frac{1}{r}\sum_{i=1}^{r} \tilde{k}^i, \tag{15.a}$$

$$\bar{\bar{k}}^r = \frac{r}{\sum_{i=1}^{r} \frac{1}{\tilde{k}^i}}. \tag{15.b}$$

where $\tilde{k}^i$ is the apparent bulk modulus of the i^{th} realization.

The estimation of the average properties of the ensemble is taken as the average of both means:

$$\hat{k}^r = \frac{\bar{k}^r + \bar{\bar{k}}^r}{2} \tag{16}$$

By construction, we have that:

$$\bar{\bar{k}}^r \leq \hat{k}^r \leq \bar{k}^r \tag{17}$$

Equality in Eq. (17) can only be obtained when all realizations lead to identical properties. This new criterion states that the RVE is obtained when the difference between the ensemble average properties $\hat{k}^r$ and any of $\bar{k}^r$ or $\bar{\bar{k}}^r$ is within a certain tolerance of their mean:

$$\delta_{\text{av}} = \left(\frac{\hat{k}^r - \bar{\bar{k}}^r}{\hat{k}^r} \right) = \left(\frac{\hat{k}^r - \bar{k}^r}{\hat{k}^r} \right) \leq tol \tag{18}$$

Isotropy criterion (new): This last criterion investigates if a single isotropic microstructure can provide accurate estimations of the effective properties. For this purpose, particular isotropic microstructures, within a tolerance, were searched for among all generated volume elements. The criterion states:

$$\delta_{iso} = \max\left(\left|\Lambda\right|\right) \leq tol\,, \tag{19}$$

where Λ is calculated using Eq. (10). The RVE consists of the smallest volume element which satisfies Eq. (19).

3.2 Determination algorithm

Each RVE determination Method (M) was formed by combining an ensemble size criterion with a volume size criterion. Table 1 lists all methods that were used in this study. For all methods involving two criteria, the main algorithm is:

1- Set the microstructure parameters: volume fraction, aspect ratio, elastic properties of constituents, tolerance and initial number of fibers represented in the volume element.

2- Generate and solve random realizations until Criterion A is satisfied.

3- If Criterion B is satisfied, the RVE is found;

   Else, increase the number of fibers and repeat from step 2.

It is important to note that only $M_{\zeta_{con}\,\delta_{stab}}$ and $M_{\zeta_{iso}\,\delta_{stab}}$, including the stability criterion based on the convergence rate of the effective properties, necessarily require sequential increments of the number of fibers. However, an incremental approach was conducted for all methods in order to determine the smallest RVE possible. The estimated smallest RVE, for all methods, would have the least accurate effective properties. Such

an approach will help conduct a more rigorous analysis of the validity of the different methods.

As for $M_{\delta_{iso}}$, all generated volumes were individually tested to find isotropic microstructures, as per Eq. (19). The RVE size was considered as the volume element with the fewest fibers that satisfies the isotropy criterion δ_{iso}. The objective of $M_{\delta_{iso}}$ is not to test another determination criterion, but rather to investigate if a single isotropic microstructure is equivalent to a RVE, within a tolerance.

4 Numerical method

4.1 Numerical simulation

More than 1200 periodic microstructures were generated in MATLABR2009a using a new modified RSA scheme presented in Appendix A. Figure 1 presents a microstructure generated using the modified RSA scheme containing 50 randomly oriented fibers of aspect ratio 50 with a 5% volume fraction. The geometries were meshed in ANSYS v12.0 using 10 nodes tetrahedron elements and solved in Abaqus/Standard v.6.10 under 6 different cases of displacement based periodic boundary conditions as stated in Eq. (7), resulting in a total of more than 7200 FE analyses. FE models contained more than 12 million nodes for volumes containing 40 fibers with an aspect ratio of 60. Computations were performed on an IBM X server 7145-AC1 with 1.5 TB RAM and parallelized over 6 to 12 XEON X7550 cores.

4.2 Material properties

A high contrast of elastic properties of ~300, for the bulk and shear moduli of the fibers over that of the matrix, was fixed in order to submit the RVE determination methods to a rigorous case typical of nanocomposite materials. The constituent properties, listed in Table 2, are similar to those of an epoxy matrix reinforced by single-walled carbon nanotube bundles [37].

5 Results and discussions

5.1 Convergence of the RVE

Figures 2 a) and b) show the evolution of the ensemble mean bulk and shear moduli, respectively, for two aspect ratios of 20 and 30 and several number of fibers as a function of the number of realizations in the ensemble. The apparent properties shown in Figures 2 a) and b) were computed using Eq. (8) and (15.a). The properties in all figures are normalized with respect to that of the matrix, while the number of fibers represented in a volume is denoted by n and the fibers aspect ratio by AR. The bulk and shear moduli in Figures 2 a) and b) show similar trends. The confidence interval for all microstructures narrows as more realizations are included in the average properties. Volumes with fewer fibers are shown to have more scattering (i.e., larger confidence intervals) and usually required more realizations to satisfy the confidence criterion of Eq. (9). For very few fibers in the volume (e.g., AR20n1 or AR30n10), it can be observed that the mean apparent properties, even after several realizations, are still distant apart from that

observed for larger numbers of fibers (e.g., AR20*n*30 or AR30*n*30). This is a reproduction of the bias that Kanit *et al.* [8] have observed for small volumes, once again showing the importance of determining effectively the RVE.

Figures 3 a) and b) show the evolution of the normalized mean bulk and shear moduli, respectively, for increasing number of fibers. Each point represents not a single realization but the ensemble of realizations that were computed. The solid lines with downward pointing triangles represent the arithmetic mean elastic properties obtained using Eq. (15.a) and the dashed lines with empty circles represent the harmonic mean elastic properties computed using Eq. (15.b). Both means get closer to each other as the number of fibers increases. For AR < 20, the means quickly stabilize; however for higher AR the curves show a lower convergence rate and required larger volumes to stabilize. The higher the aspect ratio, the more difficult it was to generate microstructures with a high number of fibers. Usually, the last point of each curve in Figure 3 was the largest number of fibers that was practically possible to generate/mesh/solve with the available methods and computational resources.

5.2 Ensemble size criteria analysis

This section analyzes and compares the ensemble isotropy criterion ζ_{iso} and the confidence criterion ζ_{iso}. To test both criteria, we introduce the ensemble mean property error with respect to that of the whole population of possible microstructures that have the same number of fibers:

$$\zeta = \frac{\left| \overline{k}^{r} - \overline{k}^{r_{\text{tot}}} \right|}{\overline{k}^{r_{\text{tot}}}}, \tag{20}$$

where r_{tot} is very large. Therefore, ζ provides a rigorous comparison basis for the ensemble size criteria, namely, the confidence criterion ζ_{con} and the isotropy criterion ζ_{iso}. Figure 4 shows the evolution of ensemble number of realizations criteria errors ζ_{con} and ζ_{iso} computed using Eq. (9) and (13), respectively, and the mean property error ζ using Eq. (20) as a function of the number of realizations for microstructures with 10 fibers of aspect ratio 20 at 5% volume fraction and for r_{tot}=150 (i.e., 150 realizations were computed). The confidence criterion ζ_{con} is close to the mean property error ζ, both around 1% even for a low number of realizations. The ensemble isotropy criterion yields larger error values. Most importantly, the isotropy error ζ_{iso} does not vanish when increasing the ensemble's number of realizations. Same trends were observed for other aspect ratios. This indicates that the ensemble isotropy criterion ζ_{iso} is too strict and cannot always determine ensemble sizes. It is concluded that this criterion is not ideal for the smallest RVE ensemble size determination.

5.3 Volume size criteria analysis

To analyze the property stability criterion δ_{stab}, the deviation criterion δ_{dev} and the averaging variations criterion δ_{av}, we introduce the effective property error with respect to the 'exact' effective properties of very large volumes:

$$\delta = \frac{\left| \overline{k}_n - \overline{k}_{n_{\max}} \right|}{\overline{k}_{n_{\max}}}, \tag{21}$$

where $n_{\max}$ indicates the largest volume size that was computed for a given aspect ratio, with enough realizations to satisfy the confidence criterion ζ_{con}. For AR ≤ 30, volume elements containing $n_{\max} = 80$ fibers were simulated and very low scattering of the effective properties was observed and both arithmetic and harmonic means were almost identical, as seen in Figure 3. We hereby assume that those largest volume sizes of $n_{\max} = 80$ simulated for AR ≤ 30 provide an accurate estimation of the effective properties. The results of those largest volume sizes are referred to as 'exact properties' and are used to validate the estimated effective properties of all methods listed in Table 1. Figure 5 shows the volume size criteria δ_{stab}, δ_{dev} and δ_{av} computed with Eq. (13), (14) and (18) and the effective property error δ computed with Eq. (21) where $n_{\max} = 80$ at different volume sizes *n* for AR = 30. For each volume size, all errors have been computed using the same ensemble of realizations that satisfied the confidence criterion ζ_{con}. For the stability criterion in Eq. (13), the number of fibers step was taken as $\Delta n = 10$. In Figure 5, the deviation criterion δ_{dev} was lower than the 5% tolerance threshold even for the smallest volume size including only one single fiber. In contrast, the effective property error δ is larger and is over the 5% tolerance threshold for the smallest volume size. This observation suggests that the deviation criterion δ_{dev}

determines biased RVEs. Herein, a biased RVE designates a RVE which has effective properties errors that exceed the prefixed tolerance. The stability criterion δ_{stab} shows good agreement with the effective property error δ only for the smallest volume size. However, the stability criterion δ_{stab} decreases very quickly with increasing volume sizes. For volume sizes above one single fiber, effective property errors δ are exceedingly larger suggesting that the stability criterion δ_{stab} determines biased RVEs. The only criterion that is shown to be able to generate non-biased RVEs is the proposed averaging variation criterion δ_{av}. The averaging variation criterion shows very good agreement with the effective property error. A similar trend was observed for all aspect ratios AR≤30.

5.4 RVE parameters

Following the RVE determination methods listed in Table 1, the RVE parameters (n_{RVE}, r_{RVE}) were determined, for $tol = 5\%$, and are listed in Tables 3 and 4 for the bulk and shear moduli, respectively. Other tolerance values were tested and are presented in Section 5.6. The same microstructure realizations were used for all determination methods investigated. It is observed in Tables 3 and 4 that $M_{\delta_{iso}}$ based on microstructure isotropy criterion δ_{iso}, as well as all methods that include the ensemble isotropy criterion ζ_{iso}, i.e. $M_{\zeta_{iso}\,\delta_{stab}}$, $M_{\zeta_{iso}\,\delta_{dev}}$ and $M_{\zeta_{iso}\,\delta_{av}}$, have not been able to find RVEs for AR > 20. Moreover, the results in Figures 3 a) and b) suggest that for an aspect ratio of 30, for example, the RVE should be reached as the property is seen to have converged. This confirms that the ensemble isotropy criterion ζ_{iso} and the single microstructure isotropy

criterion are too strict. The last column in Table 3 shows the number of isotropic realizations found over the total number of realizations computed at that particular volume size. It can be concluded that finding isotropic realizations using δ_{iso} is not a trivial process. In contrast, the methods including the confidence criterion ζ_{con}, i.e. $M_{\zeta_{con}\,\delta_{stab}}$, $M_{\zeta_{con}\,\delta_{dev}}$ and $M_{\zeta_{con}\,\delta_{av}}$, reach the RVE for all volume sizes. It is also observed that $M_{\zeta_{con}\,\delta_{av}}$, including the averaging variation criterion delivers the largest RVE sizes, whereas $M_{\zeta_{con}\,\delta_{dev}}$ generally yielded smallest RVEs containing one single fiber.

5.5 Effective properties

Tables 5 and 6 present for all methods the estimated effective bulk and shear moduli, respectively. Also included in Tables 5 and 6 are the 'exact properties' determined using the larger number of fibers $n_{max} = 80$ for ARs up to 30. The errors of the estimated effective properties of the different methods with respect to the 'exact properties' are also presented in Tables 5 and 6.

For all methods that include the ensemble isotropy criterion ζ_{iso}, i.e. $M_{\zeta_{iso}\,\delta_{stab}}$, $M_{\zeta_{iso}\,\delta_{dev}}$ and $M_{\zeta_{iso}\,\delta_{av}}$, whenever the RVE was found, the corresponding effective properties are relatively accurate (error under 5%), with the lowest errors found when combined with the averaging criterion δ_{av} in $M_{\zeta_{iso}\,\delta_{av}}$ (1% error or lower).

As for methods that include the confidence criterion ζ_{con}, $M_{\zeta_{con}\,\delta_{stab}}$ and $M_{\zeta_{con}\,\delta_{dev}}$ based on the stability criterion δ_{stab} and the deviation criterion δ_{dev}, respectively, produce errors, with respect to 'exact properties', that increase with higher aspect ratio values. The errors reach 6% and 10% at AR= 30 for $M_{\zeta_{con}\,\delta_{stab}}$ and $M_{\zeta_{con}\,\delta_{dev}}$, respectively. In contrast, RVE volume sizes determined as per $M_{\zeta_{con}\,\delta_{av}}$ show very low errors (1% or lower) for aspect ratios up to 30.

The realizations which were found to satisfy the isotropy criterion δ_{iso} provided exceedingly accurate effective properties with practically zero errors with respect to 'exact properties', as seen in Tables 5 and 6 . This indicates that for the case of ROFRCs under study, whenever an isotropic realization is found, it can serve as an accurate RVE.

To assess the estimated effective properties for AR≥30, they are compared with FE results for all the number of fibers simulated as in Figures 6.a) and b) for the bulk and shear moduli, respectively. It can be seen in Figures 6.a) and b) that, for $M_{\zeta_{con}\,\delta_{stab}}$ and $M_{\zeta_{con}\,\delta_{dev}}$, the determined RVEs for all aspect ratios show a bias. The stability criterion δ_{stab} induced bias in $M_{\zeta_{con}\,\delta_{stab}}$ can be explained by the fact that the effective properties of ROFRCs with high aspect ratios of fibers have a low converging rate, lower than the 5% tolerance, with increasing number of fibers. However, the stability criterion is expected, in principle, to identify accurate RVEs if the tolerance was arbitrarily small. Therefore, to be able to identify the real RVE using the properties stability criterion, a convergence study has also to be performed on the choice of tolerance. The choice of tolerance values is discussed in the following section. Also seen in Figures 6.a) and b),

$M_{\zeta_{con}\,\delta_{av}}$ is the only method to provide realistic estimations of effective properties for all aspect ratios.

Another substantial benefit of $M_{\zeta_{con}\,\delta_{av}}$ is that it does not necessarily require a series of computations on subsequent volumes sizes to determine the RVE. If the first guess volume size satisfies Eq. (13), there is no need for incrementing the volume size. In contrast, the methods based on the stability criterion require a series of computations for increasing volume sizes. Therefore, $M_{\zeta_{con}\,\delta_{av}}$ helps reducing the computational time of the whole RVE determination process.

5.6 Tolerance analysis

The real errors of the estimated effective properties of all methods are that which are calculated with respect to the 'exact properties'. Even though the different tolerance definitions have different meanings than that of the real error, it would be very useful that a method estimates effective properties yielding errors, with respect to the exact results, which are equal or lower than the initial tolerance value. Such a method would ensure that the real errors of effective properties estimations are lower than the chosen tolerance value. To analyze the effect of tolerance choice, $M_{\zeta_{con}\,\delta_{stab}}$, $M_{\zeta_{con}\,\delta_{dev}}$ and $M_{\zeta_{con}\,\delta_{av}}$ were performed for tolerances varying from 1% to 5%. Figure 7 presents the estimated effective properties errors, with respect to the 'exact properties', using the three RVE determination methods ($M_{\zeta_{con}\,\delta_{stab}}$, $M_{\zeta_{con}\,\delta_{dev}}$ and $M_{\zeta_{con}\,\delta_{av}}$) for fibers aspect ratio of 30. The dashed line represents the case of equality between the tolerance and the error value. An appropriate RVE determination method should yield errors lower or equal to the

tolerance value. $M_{\zeta_{con}\,\delta_{stab}}$ and $M_{\zeta_{con}\,\delta_{dev}}$ show errors larger than the tolerance value. The $M_{\zeta_{con}\,\delta_{av}}$, based on the confidence and averaging variation criteria, is the only method to show acceptable errors for all tolerance choices.

5.7 RVE size correlation

Here we attempt to investigate the existence of a correlation between any RVE related parameter (e.g. RVE edge length) and geometrical parameters of the microstructure (e.g. aspect ratio of fibers). Any correlation could provide a firsthand tool for a quick estimation of the RVE size without performing any FE computations. Harper *et al.* [29] determined the RVEs of randomly oriented carbon fiber composites simplified in 2D representations using an embedded cell FE approach. They observed that the results always converged at the same RVE edge length which is about 4 times larger than the fiber length (tested for three aspect ratios: 1.8, 3.6 and 7.1 and two volume fractions: 30% and 50%). Figure 8 shows the RVE edge length normalized with respect to the fiber edge length as a function of the aspect ratio. All results are those of the RVEs determined using $M_{\zeta_{con}\,\delta_{av}}$ for both bulk and shear moduli for a tolerance of 5%. The RVE normalized edge length is shown to be constant for aspect ratios of 10 or larger. However, the RVE normalized edge length value (around 0.5) is strictly lower than the normalized RVE length value of 4 that was stated by Harper et *al.* [29]. This finding, based on 3D simulations and rigorous RVE determination, can provide guidelines to estimate the RVE size for a specified aspect ratio without any computation, reducing further the RVE determination computational costs. It should be noted, however, that this

value is restricted to the mechanical properties simulated. It is expected that lower contrasts between the constituents' properties or lower volume fractions should lead to smaller RVE sizes.

6 Conclusions

Several RVE determination methods have been presented and tested for the determination of both RVE parameters (n_{RVE}, r_{RVE}). The RVE was determined using different criteria separated in two sub-categories: ensemble size criteria and volume size criteria. The most important conclusions of the study are summarized in the following:

- The property stability criterion, which is the most commonly used criterion for RVE determination, as well as the standard deviation criterion are inappropriate for determining RVEs of ROFRCs with high aspect ratios of fibers.
- Single microstructures that yield isotropic elasticity tensors, within a tolerance, yield accurate effective properties. However, it becomes very difficult to obtain isotropic microstructures for high aspect ratios. This criterion could be added as an exit condition into a RVE determination algorithm in order to reduce further the computational time if, by chance, a realization meeting this criterion was obtained.
- The newly proposed averaging criterion computes accurate estimations of ROFRCs effective properties, within a given tolerance. Moreover, the averaging criterion does not necessitate the computation of the apparent properties at different volume sizes to study the convergence, as the stability criterion does. This reduces substantially the computational cost related to the RVE determination process.

- The RVE edge length was found to be around half the fiber length for aspect ratios larger than 10, allowing firsthand quick estimations of RVE sizes.

The above-mentioned findings have two major impacts on existing and future works:

- The validity of all studies relying on the property stability criterion is under question. In fact, the criterion was also not assessed, to the author's knowledge, for other types of microstructures.
- ROFRCs RVE determination cost is reduced due to the new proposed criterion and to the RVE size firsthand estimation, hence guiding the way towards numerical homogenization of high cost microstructures such as nanocomposites with very high aspect ratio reinforcements.

However, in order to achieve higher volume fractions, and especially larger aspect ratios, further advancements should be made in the microstructure generation method. In addition, cost-efficient mesh-free techniques should be sought for solving volume elements containing fibers of larger aspect ratios that are impossible to solve with the current computational resources.

Acknowledgment

The work of Hadi Moussaddy was funded by the National Science and Engineering research Council of Canada (NSERC). Most of the computations were performed on supercomputers financed by the Canadian Foundation for Innovation (CFI) and the NSERC. These computers are hosted by the Fluid Dynamics Laboratory (LADYF) of École Polytechnique de Montréal.

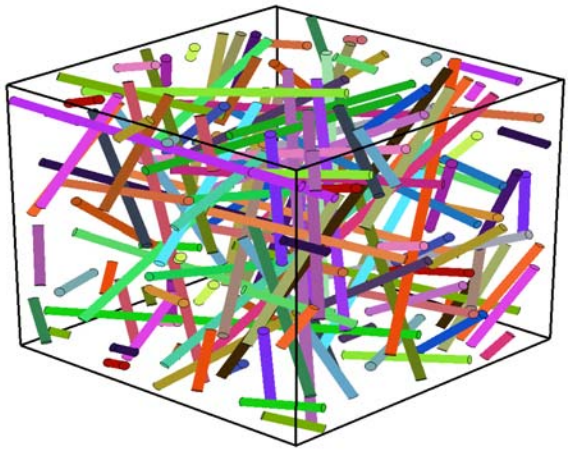

Fig. 1. Generated microstructure using the modified RSA method with 50 randomly oriented fibers having an aspect ratio of 50 and 5% volume fraction.

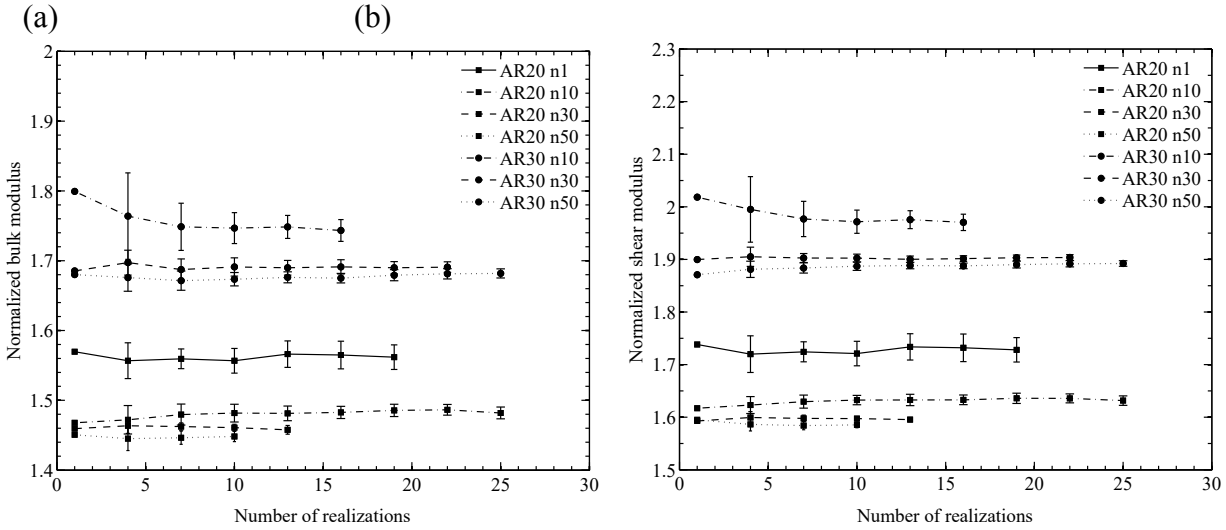

Fig. 2. Normalized average apparent properties with respect of that of the matrix as a function of the number of realizations for fiber Aspect Ratios (AR) 20 and 30 and different number of fibers (n) ranging from 1 to 50. a) Normalized bulk modulus; b) Normalized shear modulus. The error bars represent a 95% confidence interval on the mean value.

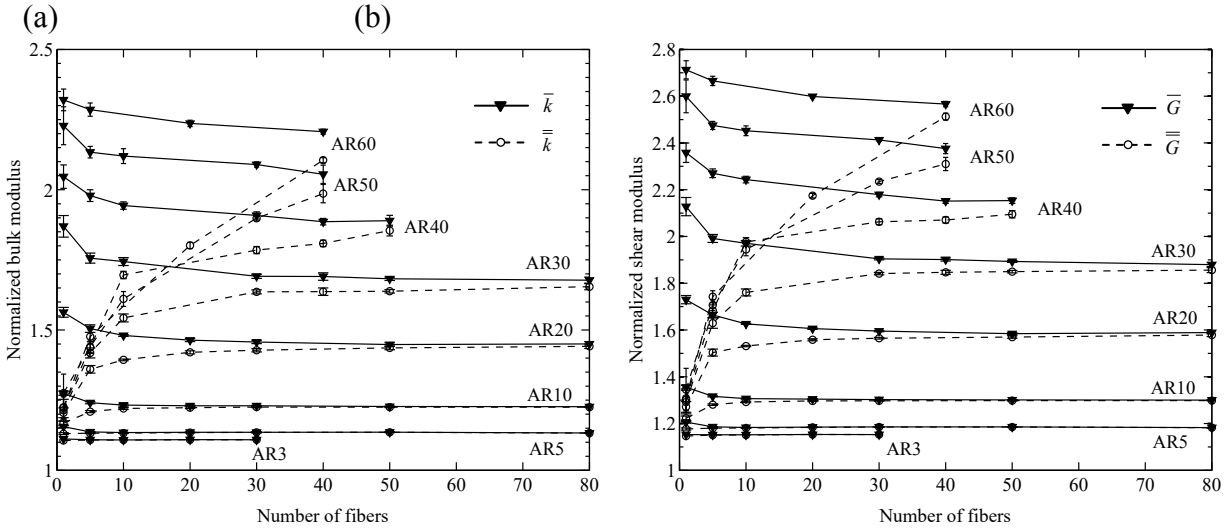

Fig. 3. Normalized average apparent properties with respect of that of the matrix as a function of the number of fibers for different Aspect Ratios (AR). a) Normalized bulk modulus; b) Normalized shear modulus. The error bars represent a 95% confidence interval on the mean value.

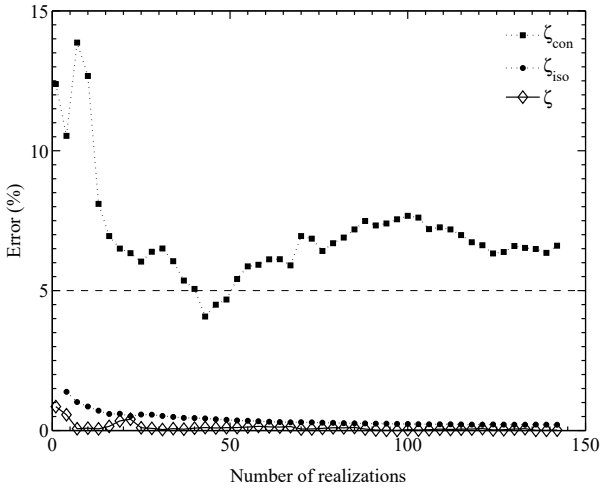

Fig. 4. Evolution of the ensemble number of realizations criteria errors ζ_{con}, ζ_{iso} and ζ expressed in Eq. (9), (10) and (20), respectively, as a function of the number of realizations in the ensemble for 10 fibers of aspect ratio 20. The dashed line represents the tolerance threshold of 5%.

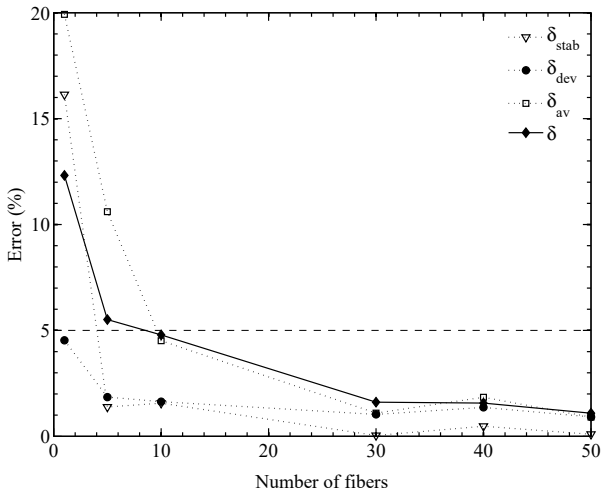

Fig. 5. Evolution of the volume size criteria errors δ_{stab}, δ_{dev}, δ_{av} and δ expressed in Eq. (13), (14), (18) and (21), respectively, as a function of the number of fibers represented for AR = 30. The dashed line represents the tolerance threshold of 5%.

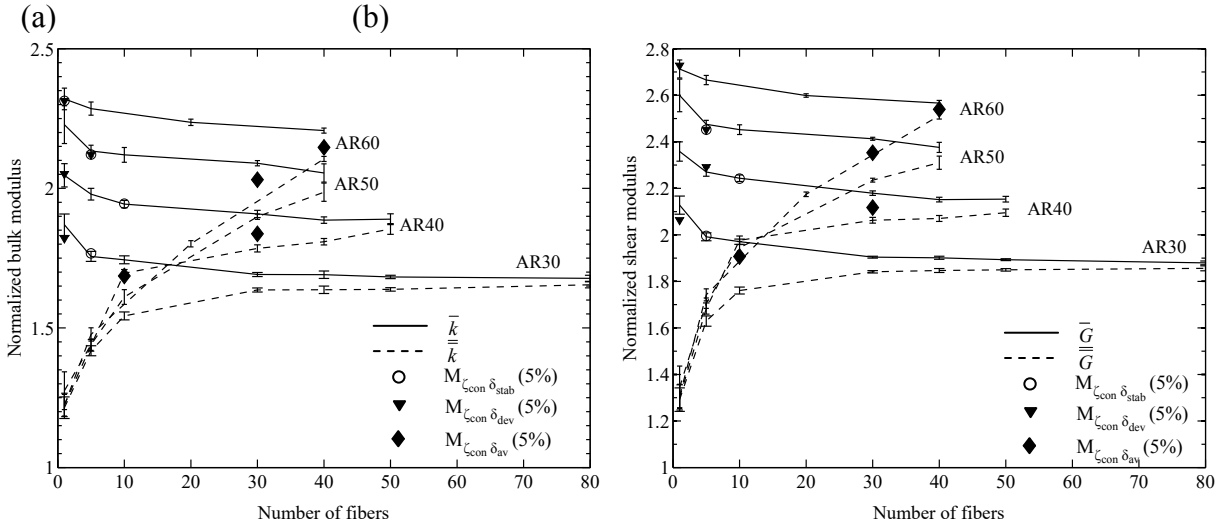

Fig. 6. Normalized properties with respect of that of the matrix as a function of the number of fibers and the RVE results using methods $M_{\zeta_{con}\,\delta_{stab}}$, $M_{\zeta_{con}\,\delta_{dev}}$ and $M_{\zeta_{con}\,\delta_{av}}$ at 5% tolerance. a) Normalized bulk modulus; b) Normalized shear modulus. The error bars represent a 95% confidence interval on the mean value.

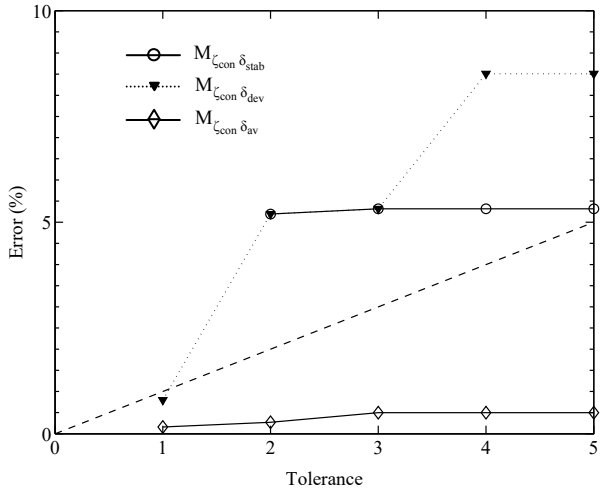

Fig. 7. Relative errors of the effective bulk modulus of RVEs determined using methods $M_{\zeta_{con}\,\delta_{stab}}$, $M_{\zeta_{con}\,\delta_{dev}}$ and $M_{\zeta_{con}\,\delta_{av}}$ with respect to the 'exact properties', for different values of tolerance and for AR=30. The dashed line represents the desired tolerance.

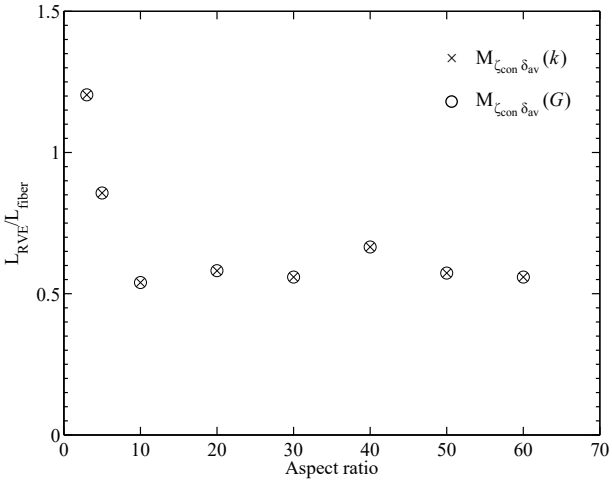

Fig. 8. Correlation between the RVE edge length $\mathbf{L_{RVE}}$ with respect to the length of the fibers represented $\mathbf{L_{fiber}}$ as a function of the fibers aspect ratio. Represented RVEs data were determined using $M_{\zeta_{con}\,\delta_{av}}$ at 5% tolerance for bulk and shear moduli.

Table 1
The RVE determination methods.

	Determination of r		**Determination of n**		**RVE**
Methods	Criterion A	Name	Criterion B	Name	Effective property
$M_{\zeta_{con}\,\delta_{stab}}$ $M_{\zeta_{iso}\,\delta_{stab}}$	$\zeta_{con} \le tol$ $\zeta_{iso} \le tol$	Confidence Ensemble isotropy	$\delta_{stab} \le tol$	Stability	$\overline{k}_{n_1}^{r_1}$ in Eq.(13)
$M_{\zeta_{con}\,\delta_{dev}}$ $M_{\zeta_{iso}\,\delta_{dev}}$	$\zeta_{con} \le tol$ $\zeta_{iso} \le tol$	Confidence Ensemble isotropy	$\delta_{dev} \le tol$	Deviation	$\overline{k}_n^r$
$M_{\zeta_{con}\,\delta_{av}}$ $M_{\zeta_{iso}\,\delta_{av}}$	$\zeta_{con} \le tol$ $\zeta_{iso} \le tol$	Confidence Ensemble isotropy	$\delta_{av} \le tol$	Averaging	$\hat{k}_n^r$
$M_{\delta_{iso}}$	NA	NA	$\delta_{iso} \le tol$	Isotropy	$\tilde{k}$

Table 2
Materials properties in GPa.

	Bulk modulus	Shear modulus
Matrix	1.67	0.77
Fibers	500	231

Table 3
RVE volume sizes *n* and number of realizations *r* for the bulk modulus at different aspect ratios for various determination Methods (M) with 5% tolerance. The last column indicates how many isotropic realizations were found over the ensemble size. When no RVE parameters are given, the RVE was not found.

	$M_{\zeta_{con}\,\delta_{stab}}$		$M_{\zeta_{iso}\,\delta_{stab}}$		$M_{\zeta_{con}\,\delta_{dev}}$		$M_{\zeta_{iso}\,\delta_{dev}}$		$M_{\zeta_{con}\,\delta_{av}}$		$M_{\zeta_{iso}\,\delta_{av}}$		$M_{\delta_{iso}}$	
AR	*n*	*r*	*n*	*r*	*n*	*r*	*n*	*r*	*n*	*r*	*n*	*r*	*n*	r/r_{tot}
3	1	5	1	5	1	5	1	5	1	5	1	5	1	2/30
5	5	5	5	5	1	5	1	6	1	5	1	6	5	2/20
10	5	5	5	5	1	5	1	13	1	5	5	5	10	3/27
20	5	5	--	--	1	5	10	38	5	5	20	26	--	--
30	5	5	--	--	1	6	--	--	10	5	--	--	--	--
40	10	5	--	--	1	9	--	--	30	5	--	--	--	--
50	5	5	--	--	5	5	--	--	30	5	--	--	--	--
60	1	7	--	--	1	7	--	--	40	5	--	--	--	--

Table 4
RVE volume sizes *n* and number of realizations *r* for the shear modulus at different aspect ratios for various determination Methods (M) with 5% tolerance. The last column indicates how many isotropic realizations were found over the ensemble size. When no RVE parameters are given, the RVE was not found.

	$M_{\zeta_{con}\,\delta_{stab}}$		$M_{\zeta_{iso}\,\delta_{stab}}$		$M_{\zeta_{con}\,\delta_{dev}}$		$M_{\zeta_{iso}\,\delta_{dev}}$		$M_{\zeta_{con}\,\delta_{av}}$		$M_{\zeta_{iso}\,\delta_{av}}$		$M_{\delta_{iso}}$	
AR	*n*	*r*	*n*	*r*	*n*	*r*	*n*	AR	*n*	*r*	*n*	*r*	*N*	*R*
3	1	5	1	5	1	5	1	5	1	5	1	5	1	2/30
5	5	5	5	5	1	5	1	6	1	5	1	6	5	2/20
10	5	5	5	5	1	5	1	13	1	5	5	5	10	3/27
20	5	5	--	--	1	5	10	38	5	5	20	26	--	--
30	5	5	--	--	1	6	--	--	10	5	--	--	--	--
40	10	5	--	--	5	5	--	--	30	5	--	--	--	--
50	5	5	--	--	5	5	--	--	30	5	--	--	--	--
60	--	--	--	--	1	15	--	--	40	5	--	--	--	--

Table 5
RVE effective normalized bulk modulus at different aspect ratios for various determination Methods (M) with 5% tolerance. When no properties are given, the RVE was not found. The errors are computed in respect to the 'exact' results (final column).

	$M_{\zeta_{con}\,\delta_{stab}}$		$M_{\zeta_{iso}\,\delta_{stab}}$		$M_{\zeta_{con}\,\delta_{dev}}$		$M_{\zeta_{iso}\,\delta_{dev}}$		$M_{\zeta_{con}\,\delta_{av}}$		$M_{\zeta_{iso}\,\delta_{av}}$		$M_{\delta_{iso}}$		**Exact**
AR	k/k_m	*er.*	k/k_m	*er.*	k/k_m	*er.*	k/k_m	*er.*	k/k_m	*er.*	k/k_m	*er.*	k/k_m	*er.*	k/k_m
3	1.11	0%	1.11	0%	1.11	0%	1.11	0%	1.11	0%	1.11	0%	1.11	0%	1.11
5	1.14	0%	1.14	0%	1.15	1%	1.15	2%	1.14	0%	1.14	0%	1.13	0%	1.13
10	1.24	2%	1.24	2%	1.27	4%	1.27	4%	1.22	0%	1.22	0%	1.22	0%	1.23
20	1.51	5%	--	--	1.56	7%	1.48	2%	1.46	1%	1.44	1%	--	--	1.45
30	1.77	6%	--	--	1.82	9%	--	--	1.69	1%	--	--	--	--	1.68
40	1.94	--	--	--	2.03	--	--	--	1.84	--	--	--	--	--	--
50	2. 12	--	--	--	2. 12	--	--	--	2.03	--	--	--	--	--	--
60	2.31	--	--	--	2.31	--	--	--	2.15	--	--	--	--	--	--

a

Table 6
RVE effective normalized shear modulus at different aspect ratios for various determination Methods (M) with 5% tolerance. When no properties are given, the RVE was not found. The errors are computed in respect to the 'exact' results (final column).

	$M_{\zeta_{con}\,\delta_{stab}}$		$M_{\zeta_{iso}\,\delta_{stab}}$		$M_{\zeta_{con}\,\delta_{dev}}$		$M_{\zeta_{iso}\,\delta_{dev}}$		$M_{\zeta_{con}\,\delta_{av}}$		$M_{\zeta_{iso}\,\delta_{av}}$		$M_{\delta_{iso}}$		**Exact**
AR	G/G_m	*er.*	G/G_m	*er.*	G/G_m	*er.*	G/G_m	*er.*	G/G_m	*er.*	G/G_m	*er.*	G/G_m	*er.*	G/G_m
3	1.15	0%	1.15	0%	1.15	0%	1.15	0%	1.15	0%	1.15	0%	1.15	0%	1.15
5	1.18	0%	1.18	0%	1.20	1%	1.20	2%	1.19	0%	1.19	0%	1.18	0%	1.18
10	1.32	2%	1.32	2%	1.35	4%	1.36	4%	1.29	1%	1.29	0%	1.30	0%	1.30
20	1.66	5%	--	--	1.72	8%	1.63	2%	1.59	0%	1.58	0%	--	--	1.59
30	2.00	6%	--	--	2.06	10%	--	--	1.91	1%	--	--	--	--	1.88
40	2.24	--	--	--	2.29	--	--	--	2.12	--	--	--	--	--	--
50	2.45	--	--	--	2.45	--	--	--	2.35	--	--	--	--	--	--
60	--	--	--	--	2.73	--	--	--	2.54	--	--	--	--	--	--

References

[1] E. Ghossein and M. Levesque, "A fully automated numerical tool for a comprehensive validation of homogenization models and its application to spherical particles reinforced composites," *International Journal of Solids and Structures,* vol. 49, pp. 1387-1398, 2012.

[2] C. L. Tucker Iii and E. Liang, "Stiffness predictions for unidirectional short-fiber composites: Review and evaluation," *Composites Science and Technology,* vol. 59, pp. 655-671, 1999.

[3] H. R. Lusti and A. A. Gusev, "Finite element predictions for the thermoelastic properties of nanotube reinforced polymers," *Modelling and Simulation in Materials Science and Engineering,* vol. 12, pp. S107-S119, 2004.

[4] B. Mortazavi*, et al.*, "Modeling of two-phase random composite materials by finite element, Mori–Tanaka and strong contrast methods," *Composites Part B: Engineering,* vol. 45, pp. 1117-1125, 2013.

[5] H. J. Böhm*, et al.*, "Multi-inclusion unit cell models for metal matrix composites with randomly oriented discontinuous reinforcements," *Computational Materials Science,* vol. 25, pp. 42-53, 2002.

[6] S. Kari*, et al.*, "Numerical evaluation of effective material properties of randomly distributed short cylindrical fibre composites," *Computational Materials Science,* vol. 39, pp. 198-204, 2007.

[7] A. A. Gusev, "Representative volume element size for elastic composites: a numerical study," *Journal of the Mechanics and Physics of Solids,* vol. 45, pp. 1449-1459, 1997.

[8] T. Kanit*, et al.*, "Determination of the size of the representative volume element for random composites: Statistical and numerical approach," *International Journal of Solids and Structures,* vol. 40, pp. 3647-3679, 2003.

[9] J. Feder, "Random sequential adsorption," *Journal of Theoretical Biology,* vol. 87, pp. 237-254, 1980.

[10] J. Talbot*, et al.*, "Random sequential addition of hard spheres," *Molecular Physics: An International Journal at the Interface Between Chemistry and Physics,* vol. 72, pp. 1397 - 1406, 1991.

[11] B. D. S. Lubachevsky, F.H.; Pinson, E.N., "Disks vs. spheres: contrasting properties of random packings," *Journal of Statistical Physics,* vol. 64, pp. 501-24, 1990.

[12] H. Altendorf and D. Jeulin, "Random-walk-based stochastic modeling of three-dimensional fiber systems," *Physical Review E,* vol. 83, p. 041804, 2011.

[13] M. Huang and Y.-m. Li, "X-ray tomography image-based reconstruction of microstructural finite element mesh models for heterogeneous materials," *Computational Materials Science,* vol. 67, pp. 63-72, 2013.

[14] T. Mori and K. Tanaka, "Average stress in matrix and average elastic energy of materials with misfitting inclusions," *Acta Metallurgica,* vol. 21, pp. 571-4, 1973.

[15] J. K. W. Sandler*, et al.*, "Ultra-low electrical percolation threshold in carbon-nanotube-epoxy composites," *Polymer,* vol. 44, pp. 5893-5899, 2003.

[16] H. Moulinec and P. Suquet, "A fast numerical method for computing the linear and nonlinear mechanical properties of composites," *Comptes Rendus de l'Academie des Sciences, Serie II (Mecanique-Physique-Chimie-Astronomie),* vol. 318, pp. 1417-23, 1994.

[17] H. Moulinec and P. Suquet, "A numerical method for computing the overall response of nonlinear composites with complex microstructure," *Computer Methods in Applied Mechanics and Engineering,* vol. 157, pp. 69-94, 1998.

[18] R. Hill, "Elastic properties of reinforced solids -- Some theoretical principles," *Journal of Mechanics and Physics of Solids,* vol. 11, pp. 357-372, 1963.
[19] K. Sab, "On the homogenization and the simulation of random materials," *European Journal of Mechanics, A/Solids,* vol. 11, pp. 585-607, 1992.
[20] R. B. Barello and M. Levesque, "Comparison between the relaxation spectra obtained from homogenization models and finite elements simulation for the same composite," *International Journal of Solids and Structures,* vol. 45, pp. 850-867, 2008.
[21] Y. Benveniste, "New approach to the application of Mori-Tanka's theory in composite materials," *Mechanics of Materials,* vol. 6, pp. 147-157, 1987.
[22] "Abaqus Analysis Users manual," *Abaqus v 6.10,* 2010.
[23] I. Lenhardt and T. Rottner, "Krylov subspace methods for structural finite element analysis," *Parallel Computing,* vol. 25, pp. 861-875, 1999.
[24] C. Farhat and F.-X. Roux, "Method of finite element tearing and interconnecting and its parallel solution algorithm," *International Journal for Numerical Methods in Engineering,* vol. 32, pp. 1205-1227, 1991.
[25] C. Farhat*, et al.*, "Transient FETI methodology for large-scale parallel implicit computations in structural mechanics," *International Journal for Numerical Methods in Engineering,* vol. 37, pp. 1945-1975, 1994.
[26] C. Farhat and F. X. Roux, "Implicit parallel processing in structural mechanics," *Computational Mechanics Advances,* vol. 2, pp. 1-124, 1994.
[27] M. Ostoja - Starzewski, "Random field models of heterogeneous materials," *International Journal of Solids and Structures,* vol. 35, pp. 2429-2455, 1998.
[28] J. Drugan and J. R. Willis, "A micromechanics-based nonlocal constitutive equation and estimates of the representative volume element size for elastic composites," *Journal of the Mechanics and Physics of Solids,* vol. 44, pp. 497-524, 1996.
[29] L. T. Harper*, et al.*, "Representative volume elements for discontinuous carbon fibre composites - Part 2: Determining the critical size," *Composites Science and Technology,* vol. 72, pp. 204-210, 2012.
[30] I. M. Gitman*, et al.*, "Representative volume: Existence and size determination," *Engineering Fracture Mechanics,* vol. 74, pp. 2518-2534, 2007.
[31] C. Pelissou*, et al.*, "Determination of the size of the representative volume element for random quasi-brittle composites," *International Journal of Solids and Structures,* vol. 46, pp. 2842-2855, 2009.
[32] H. Moussaddy*, et al.*, "Comparing finite element and analytical micromechanical modeling of randomly oriented single walled carbon nanotubes reinforced nanocomposites," presented at the 2nd Joint US-Canada Conference on Composites - American Society for Composites, 26th Annual Technical Conference: Canadian Association for Composite Structures and Materials, September 26, 2011 - September 28, 2011, Montreal, QC, Canada, 2011.
[33] D. Trias*, et al.*, "Determination of the critical size of a statistical representative volume element (SRVE) for carbon reinforced polymers," *Acta Materialia,* vol. 54, pp. 3471-3484, 2006.
[34] M. Salmi*, et al.*, "Various estimates of Representative Volume Element sizes based on a statistical analysis of the apparent behavior of random linear composites," *Comptes Rendus Mécanique,* vol. 340, pp. 230-246, 2012.

[35] S. I. Ranganathan and M. Ostoja-Starzewski, "Universal elastic anisotropy index," *Physical Review Letters,* vol. 101, p. 055504, 2008.

[36] I. Bucataru and M. A. Slawinski, "Invariant properties for finding distance in space of elasticity tensors," *Journal of Elasticity,* vol. 94, pp. 97-114, 2009.

[37] J. Z. Liu*, et al.*, "Mechanical properties of single-walled carbon nanotube bundles as bulk materials," *Journal of the Mechanics and Physics of Solids,* vol. 53, pp. 123-142, 2005.

APPENDIX A - Modified RSA

We propose an extension for the RSA algorithm in order to facilitate the generation of higher volume fractions and aspect ratios in random packings of straight fibers. In this modified algorithm, fibers are considered as straight cylinders having the same aspect ratio and same dimensions. A single modification to the RSA classical scheme is implemented when overlapping occurs, i.e. when the distance between a newly generated fiber *f2* and an existing fiber *f1* is less than the fixed minimum distance *e* between two accepted fibers.

Let the minimum distance vector from the first fiber *f1* axis to the newly generated fiber *f2* axis be noted $\mathbf{v}_{12}$. The second fiber *f2* is translated following the $\mathbf{v}_{12}$ direction to satisfy the minimum distance requirement. The vector of translation **d** is expressed by:

$$\mathbf{d} = e \ \frac{\mathbf{v}_{12}}{\left\|\mathbf{v}_{12}\right\|} \tag{A.1}$$

Following the translation, the distances between the translated fiber *f2* and all other existing fibers axes are verified. If the minimum distance is not satisfied, the fiber *f2* is removed, and a new random fiber position and orientation are generated. Using this algorithm with a zero inter-fiber minimum distance, volume fractions up to 38% and 29% were generated for ROFRCs with aspect ratios 10 and 30, respectively. Figure 1 shows an example of a ROFRC generated using the modified RSA method. The microstructure contains 50 randomly oriented fibers of aspect ratio 50 at 5% volume fraction. The

microstructure is periodic, meaning that a fiber that crosses one surface of the volume penetrates back from the opposite surface. This condition is imperative in order to obtain identical FE meshes on opposite sides and, consequently, to apply periodic boundary conditions as expressed in Eq. (1).